

Structural and spectroscopic study of NaSbR(PO₄)₃ (R = Cr, Fe, In) phases

Abderrahim Aatiq and My Rachid Tigha

Département de Chimie, Laboratoire de Physico-Chimie des Matériaux Appliqués, Université HassanII-Mohammédia, Faculté des Sciences Ben M'Sik, Avenue Idriss El harti, B.P. 7955, Casablanca, Morocco.

Crystallographic structures of the three NaSbR(PO₄)₃ (R = Cr, Fe, In) phases were determined at room temperature from X-ray powder diffraction (XRD) data using the Rietveld analysis. The three compounds belong to the Nasicon structural family. The presence of the (303) reflection in all XRD spectra of NaSbR(PO₄)₃ shows clearly that all compounds crystallise in rhombohedral system with $R\bar{3}$ space group. Na atoms are practically ordered within the two positions, 3a and 3b, of M1 sites. Structure refinements show also a partially-ordered distribution of Sb⁵⁺ and R³⁺ ions within the Nasicon framework. A Raman and Infrared spectroscopic study was used to obtain further structural information about the nature of bonding in NaSbR(PO₄)₃ (R = Cr, Fe, In) phases.

Key words: Antimony phosphate; Nasicon structure; Raman and IR spectroscopy; Rietveld analysis

a) Electronic-mail: a_aatiq@yahoo.fr Fax : +212-522 70 46 75

I. INTRODUCTION

The Nasicon-type family has been the subject of intensive research due to its potential applications as solid electrolyte, electrode material, low thermal expansion ceramics and as storage materials for nuclear waste (Hong, 1976; Padhi et al., 1997; Roy et al., 1982; Delmas et al., 1981; Woodcock et al., 1999). The structure of such materials with general formula $A_xXX'(PO_4)_3$ consists of a three-dimensional network made up of corner-sharing $X(X')O_6$ octahedra and PO_4 tetrahedra in such a way that each octahedron is surrounded by six tetrahedra and each tetrahedron is connected to four octahedral. Within the Nasicon framework, there are interconnected interstitial sites usually labelled M1 (one per formula unit) and M2 (three per formula unit) through which A cation can diffuse, giving rise to a fast-ion conductivity (Hong, 1976; Delmas et al., 1981) (Figure 1). The four such sites per formula unit can be represented by the crystallographic $[M2]_3[M1]XX'(PO_4)_3$ formula. Each M1 cavity is situated between two $X(X')O_6$ octahedra along the c-axis. Six M2 cavities with eightfold coordination are located between the $[O_3X(X')O_3M1O_3X(X')O_3]_{\infty}$ ribbons and surround the M1 cavity (Figure1).

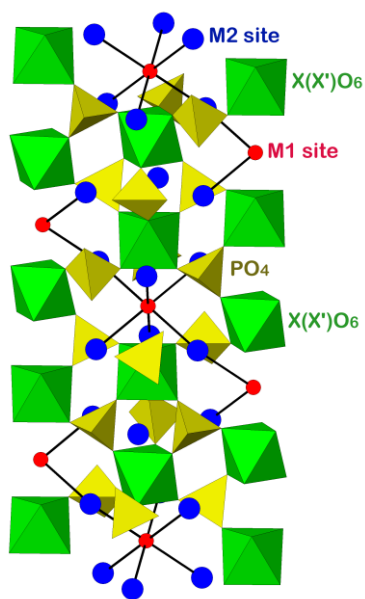


Figure 1. Crystal structure of the rhombohedral $[M2]_3[M1]XX'(PO_4)_3$ Nasicon-type.

Recently, the structural characteristics by powder X-ray diffraction (XRD) study using the Rietveld method for $A_{0.50}\text{SbFe}(\text{PO}_4)_3$ ($A = \text{Ca}, \text{Sr}$) ($R\bar{3}$ space group) and $\text{ASb}_{0.50}\text{Fe}_{1.50}(\text{PO}_4)_3$ ($R\bar{3}c$ space group) phases were realised (Aatiq, Tigha et al. 2006; Aatiq et al., 2012). In $A_{0.50}\text{SbFe}(\text{PO}_4)_3$ sample, A^{2+} ions occupied one-half of the M1 sites and the Sb^{5+} and Fe^{3+} cations are orderly distributed within the $\text{SbFe}(\text{PO}_4)_3$ framework. In a continuation of our search concerning Nasicon-like phases herein we report the results of the structural investigation by the Rietveld refinement using the XRD patterns of the three $\text{NaSbR}(\text{PO}_4)_3$ ($R = \text{Cr}, \text{Fe}, \text{In}$) phases. In order to obtain further structural information about the nature of bonding in the crystalline solids, a Raman and Infrared spectroscopic study was also undertaken.

II. EXPERIMENTAL

Syntheses of $\text{NaSbR}(\text{PO}_4)_3$ ($R = \text{Cr}, \text{Fe}, \text{In}$) phases were carried out using conventional solid-state reaction techniques. Powder crystalline samples were prepared from mixtures of carbonates Na_2CO_3 (Riedel-de Haën, 99 %), oxides Sb_2O_3 (Riedel-de Haën, 99.9 %), R_2O_3 ($R = \text{Cr}, \text{Fe}, \text{In}$) (Prolabo, 99 %) and $\text{NH}_4\text{H}_2\text{PO}_4$ (Riedel-de Haën, 99 %) in stoichiometric proportions. The mixture was heated progressively with intermittent grinding at 200°C (12h), 400°C (6h), 600°C (12h), 800°C (24h), 900°C (24h) and 1000°C (24h) in air atmosphere. The products of reaction were characterised by X-ray diffraction (XRD) at room temperature with a Panalytical X'Pert-PRO (θ -2 θ) diffractometer; ($\text{CuK}\alpha$) radiation (45 kV, 40 mA); divergence slit of 1° and antiscatter slit of 1°. The data were collected from 10 to 90° 2 θ , in steps of 0.017°, with a counting time of 30 s per step. The Rietveld refinement of the structure was performed using the Fullprof program (Rodriguez-Carvajal, 1997).

The infrared spectra are recorded in the form of KBr pellets in the wave number range 1500-400 cm^{-1} using a Bruker's VERTEX 70 spectrometer and the Raman spectra are recorded on RENISHAW 1000B spectrometer in the wave number range 100–1500 cm^{-1} . All the spectra have been recorded at room temperature.

III. RESULTS AND DISCUSSION

Analysis of the powder XRD spectra for the three $\text{NaSbR}(\text{PO}_4)_3$ ($R = \text{Cr}, \text{Fe}, \text{In}$) materials indicated that the principal peak positions of the XRD lines are similar to those observed for other Nasicon-type phases (Figure 2-4). The XRD pattern of $\text{NaSbIn}(\text{PO}_4)_3$ shows clearly the

presence of diffraction peaks, with Miller indexes $h0l$ ($l = 2n+1$) [e.g., (101) and (003) reflections] at 11.52 in two theta, characteristic of the $R\bar{3}$ space group. A rapid analysis of the two $\text{NaSbR}(\text{PO}_4)_3$ ($R = \text{Cr}, \text{Fe}$) XRD data shows the absence of the usually known (101) and (003) reflections. Therefore, in a first approximation, the structure refinement of the two last compounds is conducted in the $R\bar{3}c$ space. Obtained Rietveld refinement results show that the particularly reflection around 39.3 , in two theta, is not generated when the refinement is realised in the $R\bar{3}c$ space group (Figures 2-3). This result leads us to suspect that the real space group is rather $R\bar{3}$. In fact, as it will be shown later this last hypothesis will be confirmed by a carefully Rietveld analysis for both $\text{NaSbR}(\text{PO}_4)_3$ ($R = \text{Cr}, \text{Fe}$) phases. In the following, the structural refinement was principally based upon the previous assumptions.

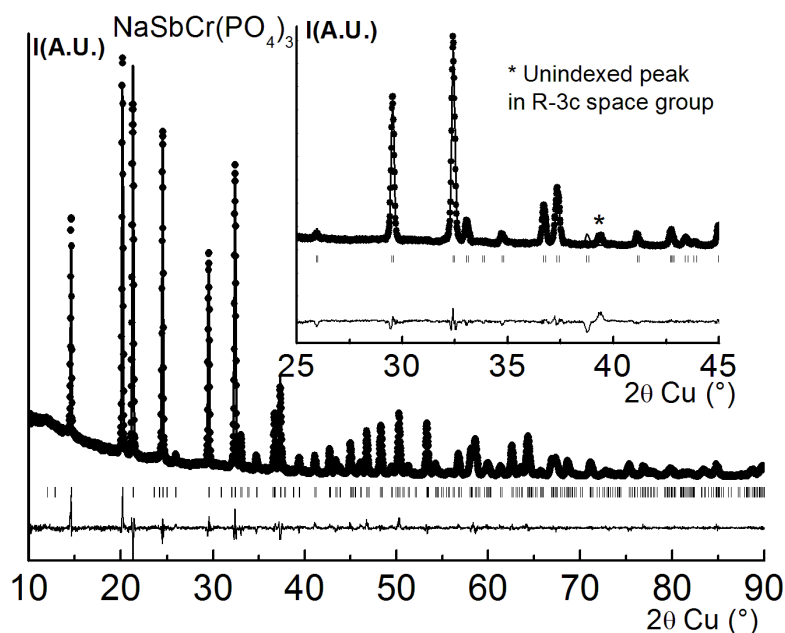


Figure 2. Experimental (●●●) calculated (—), and difference profile of the XRD pattern of $\text{NaSbCr}(\text{PO}_4)_3$. Inset shows results of refinement in $R\bar{3}c$ space group.

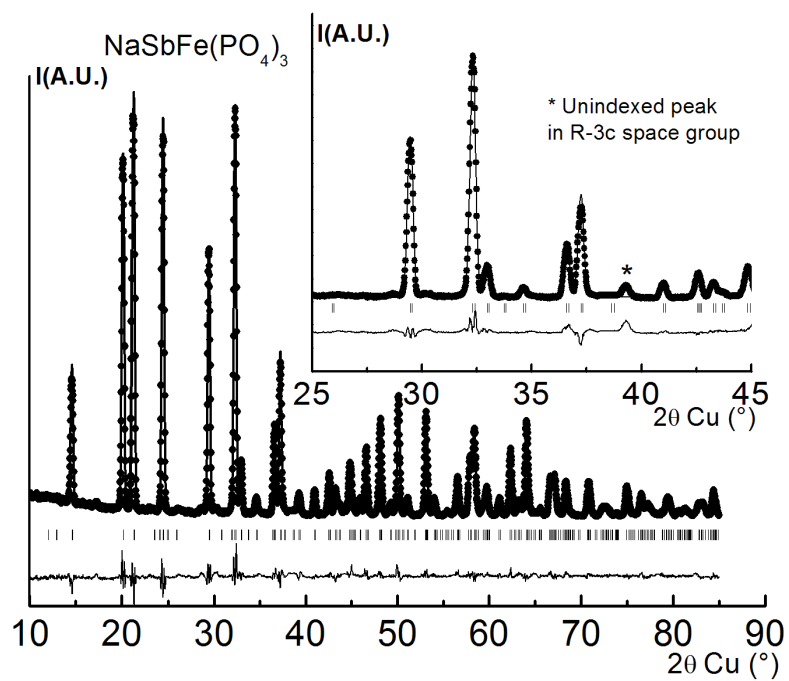


Figure 3. Experimental (●●●) calculated (—), and difference profile of the XRD pattern of $\text{NaSbFe}(\text{PO}_4)_3$. Inset shows results of refinement in $R\bar{3}c$ space group.

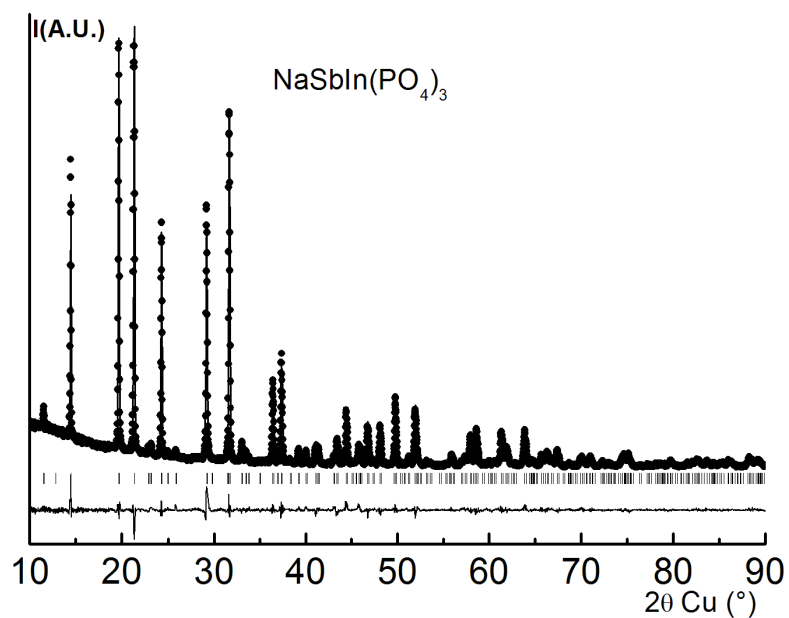


Figure 4. Experimental (●●●) calculated (—), and difference profile of the XRD pattern of $\text{NaSbIn}(\text{PO}_4)_3$.

A. Structure of NaSbR(PO₄)₃ (R = Cr, Fe) phases

Structure determination of NaSbR(PO₄)₃ (R = Cr, Fe) phases, using the Rietveld method, was therefore undertaken in two principle models. In the first, the refinement was made in R $\bar{3}$ c space group whereas in the second model the hypothesis of R $\bar{3}$ space group was verified. During the first model, initial starting parameters for the Reitveld Refinements, using R $\bar{3}$ c space group, were based on those already reported for MnFeTi(PO₄)₃ (Aatiq and Dhomm, 2006). Na atoms are distributed in the M1 site, 6c position (0 0 ~0.25), while Sb⁵⁺ and R³⁺ are supposed to reside within the framework. As shown in the inset of Figures 2 and 3, result of refinement in R $\bar{3}$ c space group was confirmed to be less appropriate. In fact, because some peaks are not generated [e.g., (303) reflections around 39.3 in two theta] this last structure refinement was dismissed. In the second model, the structural parameters of Ca_{0.50}SbFe(PO₄)₃ (R $\bar{3}$ space group) (Aatiq, Tigha et al. 2006) were used as starting parameters for the Rietveld refinement of NaSbR(PO₄)₃ (R = Cr, Fe). Refinement with Na atom distributed between the two M1(3a) and M1(3b) sites and the Sb(R) atoms within the Nasicon framework leads to best results. The final reliability factors and atomic parameters for NaSbCr(PO₄)₃ and NaSbFe(PO₄)₃ phases are summarised in Tables I and II respectively. A comparison of the experimental and calculated XRD profile is shown in Figures 2 and 3. Na-O and X-O (X = Sb(Cr) or Sb(Fe)) distances values are grouped in Table III. Obtained interatomic distances are consistent with the ionic radii values in six coordination of Na⁺, Sb⁵⁺ and R³⁺ ions (Shannon, 1976). P-O distances values match well with those typically observed in Nasicon-type phosphates. In order to have more structural information, the bond valence sum (BVS) based on bond strength analysis (Brown and Altermatt, 1985) for NaSbR(PO₄)₃ (R = Cr, Fe) were also computed. As shown in Table III, the BVS values calculated for Na, R, Sb and P sites are relatively consistent with the expected formal oxidation state of Na⁺, R³⁺, Sb⁵⁺ and P⁵⁺ ions.

Table I. Results of the Rietveld refinement of NaSbCr(PO₄)₃

Na[SbCr]_X(PO₄)₃
 Space group, R $\bar{3}$; [Z = 6, a = 8.329(1) Å, c = 22.094(2) Å; V = 1327(1) Å³]
 Profile parameters
 Pseudo-voigt function, PV = $\eta L + (1-\eta)G$; $\eta = 0.390(11)$
 Half-width parameters, U = 0.255(11), V = -0.053(6), and W = 0.015(1)
 Conventional Rietveld R-factors, R_{WP} = 8.1%; R_P = 5.9%; R_B = 4.4%; R_F = 3.0 %

Atom	Site	Wyckoff positions			B _{iso} (Å ²)	Occupancy
Na(1)	3a	0	0	0	2.6(3)	1
Na(2)	3b	0	0	0.5	2.6(3)	1
X(1) = Cr(1)/Sb(1)	6c	0	0	0.1453(3)	1.6(2)	0.56/0.44(1)
X(2) = Cr(2)/Sb(2)	6c	0	0	0.6467(3)	1.6(2)	0.44/0.56(1)
P	18f	0.2909(4)	0.0069(5)	0.2505(2)	0.6(1)	1
O(1)	18f	0.1738(6)	0.1785(6)	0.0902(5)	0.4(1)	1
O(2)	18f	0.1440(6)	0.2090(7)	0.4120(5)	0.4(1)	1
O(3)	18f	0.1970(7)	0.9968(5)	0.1897(3)	0.4(1)	1
O(4)	18f	0.9258(7)	0.1399(6)	0.3014(3)	0.4(1)	1

Table II. Results of the Rietveld refinement of NaSbFe(PO₄)₃

Na[SbFe]_X(PO₄)₃
 Space group, R $\bar{3}$; [Z = 6, a = 8.361(1) Å, c = 22.222(2) Å; V = 1345(1) Å³]
 Profile parameters
 Pseudo-voigt function, PV = $\eta L + (1-\eta)G$; $\eta = 0.488(1)$
 Half-width parameters, U = 0.135(1), V = -0.032(7), and W = 0.014(1)
 Conventional Rietveld R-factors, R_{WP} = 8.1%; R_P = 7.3%; R_B = 4.3%; R_F = 3.7%

Atom	Site	Wyckoff positions			B _{iso} (Å ²)	Occupancy
Na(1)	3a	0	0	0	3.5(4)	1
Na(2)	3b	0	0	0.50	3.5(4)	1
X(1) = Fe(1)/Sb(1)	6c	0	0	0.1450 (3)	1.5(2)	0.57/0.43(2)
X(2) = Fe(2)/Sb(2)	6c	0	0	0.6482(3)	1.5(2)	0.43/0.57(2)
P	18f	0.2901(4)	0.0022(6)	0.2508(2)	1.6(1)	1
O(1)	18f	0.1749(7)	0.1840(14)	0.0901(7)	0.7(1)	1
O(2)	18f	0.1422(8)	0.2070(6)	0.4100(5)	0.7(1)	1
O(3)	18f	0.1917(6)	0.9991(5)	0.1925(5)	0.7(1)	1
O(4)	18f	0.937(1)	0.1484(6)	0.3024(5)	0.7(1)	1

Table III. Selected interatomic distances and calculated Bond valence sum (BVS) for NaSbR(PO₄)₃ (R= Cr, Fe, In) phases

X-O distances (Å)	P-O distances (Å)	Na-O distances (Å)
Na[SbCr] _x (PO ₄) ₃		
X(1)-O(1) = 1.907(2)		
X(1)-O(3) = 1.922(3)	P-O(1) = 1.516(2)	Na(1)-O(1) = 2.475(2)
Aver.<X(1)-O> = 1.915	P-O(2) = 1.552(3)	Na(2)-O(2) = 2.482(3)
BVS(X(1)) = 5.32 (should be 4)	P-O(3) = 1.534(3)	
X(2)-O(2) = 2.016(2)	P-O(4) = 1.532(2)	BVS(Na(1)) = 0.98
X(2)-O(4) = 1.942(3)	Aver.<P-O> = 1.544	BVS(Na(2)) = 0.96
Aver.<X(2)-O> = 1.979	BVS(P) = 4.9	
BVS(X(2)) = 4.7 (should be 4)		
Na[SbFe] _x (PO ₄) ₃		
X(1)-O(1) = 1.936(2)	P-O(1) = 1.520(3)	Na(1)-O(1) = 2.502(2)
X(1)-O(3) = 1.922(3)	P-O(2) = 1.539(3)	Na(2)-O(2) = 2.520(3)
Aver.<X(1)-O> = 1.929	P-O(3) = 1.528(2)	
BVS(X(1)) = 3.8 (should be 3.9)	P-O(4) = 1.528(2)	BVS(Na(1)) = 0.90
X(2)-O(2) = 2.005(2)	Aver.<P-O> = 1.529	BVS(Na(2)) = 0.90
X(2)-O(4) = 1.985(3)	BVS(P) = 5.0	
Aver.<X(2)-O> = 1.995		
BVS(X(2)) = 4.3 (should be 4.1)		
Na[SbIn] _x (PO ₄) ₃		
X(1)-O(1) = 2.083(3)		
X(1)-O(3) = 2.078(2)	P-O(1) = 1.513(2)	Na(1)-O(1) = 2.494(2)
Aver.<X(1)-O> = 2.080	P-O(2) = 1.508(3)	Na(2)-O(2) = 2.554(3)
BVS(X(1)) = 3.9 (should be 4)	P-O(3) = 1.510(2)	
X(2)-O(2) = 2.123(3)	P-O(4) = 1.525(3)	BVS(Na(1)) = 0.90
X(2)-O(4) = 2.069(2)	Aver.<P-O> = 1.514	BVS(Na(2)) = 0.80
Aver.<X(2)-O> = 2.096	BVS(P) = 5.2	
BVS(X(2)) = 3.8 (should be 4)		

B. Structure of NaSbIn(PO₄)₃

The structural parameters of NaSbFe(PO₄)₃ ($R\bar{3}$ space group) were used as starting parameters for the Rietveld refinement of NaSbIn(PO₄)₃. Refinement with all Na atom in the two M1(3a) and M1(3b) sites and Sb(In) atoms within the Nasicon framework leads to best results ($R_B = 5.0\%$). The final reliability factors and atomic parameters for NaSbIn(PO₄)₃ are summarised in Table IV. A comparison of the experimental and calculated XRD profile is shown in Figure 4. Na-O, X-O (X = Sb(In)) and P-O distances are consistent with the ionic radii values,

in six coordination, of Na⁺, Sb⁵⁺ and In³⁺ ions (Table III). The correctness of the NaSbIn(PO₄)₃ structure was also confirmed by bond valence calculations.

Table IV. Results of the Rietveld refinement of NaSbIn(PO₄)₃

Na[SbIn] _x (PO ₄) ₃						
Space group, R $\bar{3}$; [Z = 6, a = 8.329(1) Å, c = 23.031(2) Å; V = 1383(1) Å ³]						
Profile parameters						
Pseudo-voigt function, PV = ηL + (1-η)G; η = 0.400(9)						
Half-width parameters, U = 0.136(7), V = -0.019(4), and W = 0.010(1)						
Conventional Rietveld R-factors, R _{WP} = 8.8 %; R _P = 6.4 %; R _B = 5.0 %; R _F = 3.9 %						
Atom	Site	Wyckoff positions			B _{iso} (Å ²)	Occupancy
Na(1)	3a	0	0	0	2.2(4)	1
Na(2)	3b	0	0	0.5	2.2 (4)	1
X(1) = In(1)/Sb(1)	6c	0	0	0.1460(1)	1.2(1)	1
X(2) = In(2)/Sb(2)	6c	0	0	0.6532(1)	1.4(1)	1
P	18f	0.2894(4)	-0.0063(5)	0.2524(2)	0.9(1)	1
O(1)	18f	0.1741(7)	0.1943(6)	0.0851(4)	0.2(1)	1
O(2)	18f	0.1320(6)	0.2090(8)	0.411(4)	0.2(1)	1
O(3)	18f	0.1899(5)	0.9654(5)	0.1952(3)	0.2(1)	1
O(4)	18f	0.9036(7)	0.1385(5)	0.2958(3)	0.2(1)	1

C. Raman and Infrared spectroscopy

In order to obtain further structural information about the nature of bonding in NaSbR(PO₄)₃ (R = Cr, Fe, In) crystalline solids, in this part of the paper, a Raman and Infrared (IR) spectroscopic study was undertaken. The IR spectra of the three samples are similar (Figure 5). Raman spectra of the selected NaSbFe(PO₄)₃ phase is shown in Figure 6.

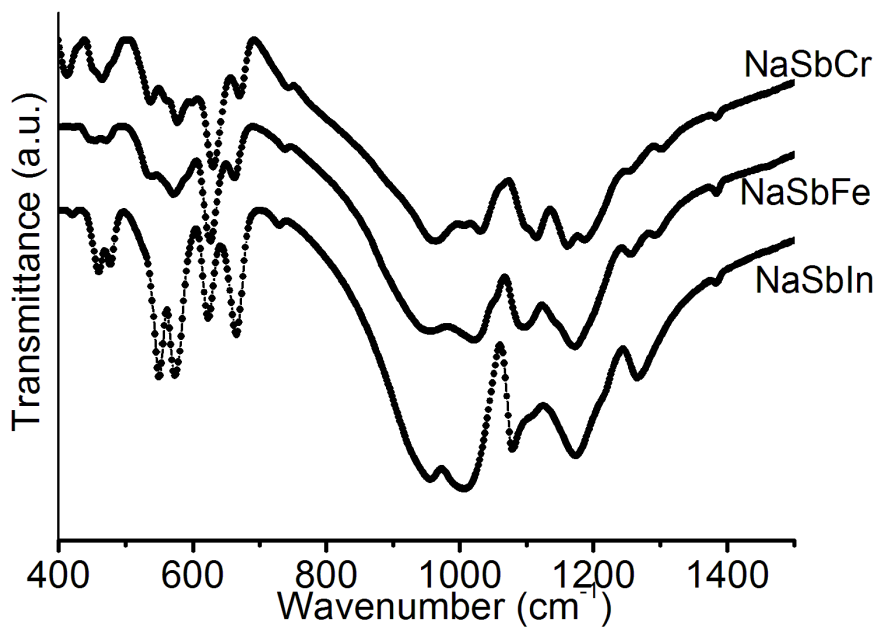


Figure 5. IR. Spectra of $\text{NaSbR}(\text{PO}_4)_3$ (R= Cr, Fe, In) phases.

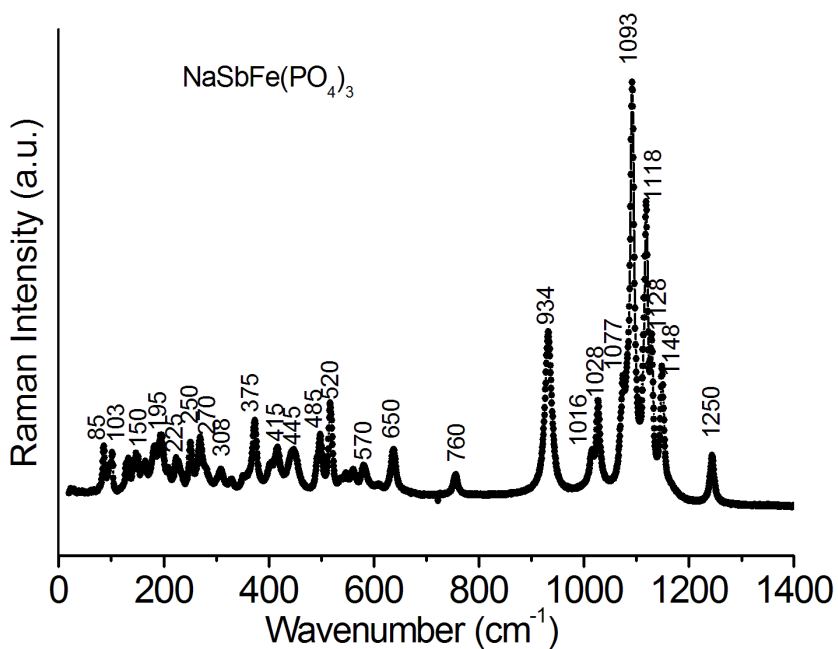


Figure 6. Raman spectrum of $\text{NaSbFe}(\text{PO}_4)_3$.

The vibration modes of $\text{NaSbR}(\text{PO}_4)_3$ ($\text{R} = \text{Cr, Fe, In}$) Nasicon phases can be assigned to internal and external modes of PO_4 tetrahedra and to lattice modes including the motions of the metallic Sb^{5+} and R^{3+} in their octahedral coordination and Na^+ ions in six coordination spheres. It is observed that phosphate group vibrations are generally strong compared to the lattice modes and metal-oxygen vibrations. According to factor group analysis, the phosphate PO_4 tetrahedra group has T_d symmetry and nine internal modes ($\Gamma_d = A_1 + E + 2F_2$).

The Raman and IR band positions of the four (ν_1, ν_2, ν_3 and ν_4) modes observed in the spectra of the $\text{NaSbR}(\text{PO}_4)_3$ ($\text{R} = \text{Cr, Fe, In}$) Nasicon series are close to those expected for Nasicon type materials. Assignments of Infrared and Raman vibration modes of the three materials are gathered in Table V. Thus, the symmetric non degenerate PO stretching modes (ν_1) are observed in the range $930\text{-}1030\text{ cm}^{-1}$ while antisymmetric doubly degenerate PO stretching (ν_2) are located in the $410\text{-}480\text{ cm}^{-1}$ range. The symmetric, triply degenerate OPO bending (ν_3) is observed between $1090\text{-}1175\text{ cm}^{-1}$ and the triply degenerate, antisymmetric and harmonic OPO bending (ν_4) is observed in the range $520\text{-}680\text{ cm}^{-1}$. Note that all the modes are Raman active except the ν_3 and ν_4 ones which are IR active only.

Table V. Assignments of Infrared and Raman vibration modes of NaSbR(PO₄)₃ (R= Cr, Fe, In) phases

NaSbCr(PO ₄) ₃	NaSbFe(PO ₄) ₃	NaSbIn(PO ₄) ₃	Assignments
IR	Raman	IR	IR
1255	1245	1256	1267
			$\nu(\text{PO}_4) / \nu(\text{MO})$ interaction
1162	1150	1172	1174
	1128		
1115	1118		1111
	1093	1097	
	1077		1079
1031	1028	1021	1006
964	934	957	956
760	760	750	740
670	650	662	665
631	638	626	623
577	570	572	573
538	520	538	550
465	485	471	477
	445	447	460
412	415	420	421
	375		
	308		
	270		
	250		
	225		
	195		
	150		
			$\nu_s(\text{Fe}^{3+}\text{-O})$
			External modes

The SbO₆ octahedra are distorted and exhibit a low symmetry. The Sb-O...P bonds existing in the three compounds have an average length of 2.00 Å. Their stretching vibrations are probably coupled with the P-O-P bending ν_4 mode. The frequencies found between 570 and 670 cm⁻¹ in Raman and IR spectra of NaSbR(PO₄)₃ (R = Cr, Fe, In) phases can be assigned empirically to Sb-O stretching modes involving Sb-O-P linkage. The same Sb-O vibrations are already observed, in the IR spectrum of SbOPO₄ at 597 and 652 cm⁻¹ (Sudarsan et al., 2002) and at 580 and 639 cm⁻¹, in the IR and Raman spectra, of Mn_{0.5}MSb(PO₄)₃ (M = Al, Fe and Cr) phases (Anantharamulu et al., 2009). Obtained results are also in good agreement with the spectroscopic study realised for Sr_{0.50}SbFe(PO₄)₃ (Aatiq et al., 2012). Note that in the three studied samples, the IR and Raman data confirm the presence of Sb⁵⁺ ions in octahedral oxygen coordination. In the lattice modes region, the translational modes of Na⁺, R³⁺ (R = Cr, Fe, In),

Sb^{5+} and PO_4^{3-} ions as well as librational modes of PO_4^{3-} ions and RO_6 , SbO_6 groups should be expected. At wavenumbers below 450 cm^{-1} strong coupling between the different bending vibrations O-P-O, O-Sb-O, Sb-O-P, Sb-O-Sb is expected (Husson et al., 1988).

The Raman bands observed at 375 and 308 cm^{-1} in $\text{NaSbFe}(\text{PO}_4)_3$ (Figure 6), could be assigned to Fe^{3+} -O stretching modes of vibrations. It can be seen that similar band positions are observed in the range $300\text{--}370\text{ cm}^{-1}$ of the $\text{Li}_3\text{Fe}_2(\text{PO}_4)_3$ Raman spectrum (Butt et al., 2004) and also at 378 and 343 cm^{-1} for $\text{Sr}_{0.50}\text{SbFe}(\text{PO}_4)_3$ phase (Aatiq et al., 2012). The low frequency modes observed below 270 cm^{-1} can be easily attributed to translational modes of the Na^+ , Sb^{5+} and $(\text{PO}_4)^{3-}$ ions.

CONCLUSION

$\text{NaSbR}(\text{PO}_4)_3$ ($\text{R} = \text{Cr, Fe, In}$) compounds are prepared and characterized by XRD, Raman and IR spectroscopy. The three samples crystallise in hexagonal lattice of the Nasicon framework with the space group $\text{R}\bar{3}$. Results of the Rietveld refinement show that the Na atoms are ordered in the Nasicon M1 site. The Na^+ cationic distribution within the two possible, 3a and 3b, positions of M1 sites may be the driving force of a partially-ordered distribution of Sb^{5+} and R^{3+} ions within the $\text{NaSbR}(\text{PO}_4)_3$ Nasicon framework. In fact, in the case of $\text{A}_{0.50}\square_{0.5}\text{SbFe}(\text{PO}_4)_3$ ($\text{A} = \text{Ca, Sr}$) phases ($\text{R}\bar{3}$ space group) where only one of the M1 is occupied [i.e., M1(3a)] and the other is empty, a practically complete ordered distribution of Sb^{5+} and Fe^{3+} ions was observed. Indeed, in order to minimise the electrostatic repulsion between neighbouring cations within the ribbons of $[\text{A}_{0.50}]_{\text{M1}(3a)}[\square_{0.5}]_{\text{M1}(3b)}\text{SbFe}(\text{PO}_4)_3$ phases two Fe^{3+}O_6 octahedra tend to juxtapose the quasi-full occupied M1(3a) sites and the unoccupied M1(3b) one have two Sb^{5+}O_6 octahedra as a neighbouring. It should be noticed that in $\text{NaSbR}(\text{PO}_4)_3$ Nasicon phases, where the two M1 site types are fully occupied by the same Na^+ cations, every Sb^{5+}O_6 and R^{3+}O_6 octahedra is situated between two Na^+O_6 octahedra [i.e. $\text{Na}(1)\text{O}_6$ and/or $\text{Na}(2)\text{O}_6$ octahedra]. Consequently, a partially ordered distribution of Sb^{5+} and R^{3+} ions within the $\text{SbR}(\text{PO}_4)_3$ Nasicon framework was normally expected. Raman and IR studies are consistent with the obtained $\text{NaSbR}(\text{PO}_4)_3$ ($\text{R} = \text{Cr, Fe, In}$) crystal structures. All spectra show characteristic PO_4 vibrations. The stretching modes of SbO_6 groups are observed at significantly higher frequency (570 and 670 cm^{-1}) than stretching modes of RO_6 groups ($\sim 375\text{ cm}^{-1}$).

Acknowledgements

The authors are grateful to Engineer in " Service Centrale d'Analyse (SCA) de l'Unités d'Appui Technique à la Recherche Scientifique (UATRS)" CNRS- Rabat, Morocco) for technical assistance; and for Centre SCA du CNRS- Rabat for making to the disposal of our Laboratory a Panalytical X'Pert-PRO diffractometer.

- Aatiq, A. and Dhoun, H. (2006). "Structure of $AFeTi(PO_4)_3$ ($A = Mn, Sr$) Nasicon-type phases," *Ann. Chim. (Cachan, Fr.)* **31**, 31-38.
- Aatiq, A., Tigha, R., Hassine, R. and Saadoune, I. (2006). "Crystallochemistry and structural studies of two newly $CaSb_{0.50}Fe_{1.50}(PO_4)_3$ and $Ca_{0.50}SbFe(PO_4)_3$ Nasicon phases," *Powder Diffr.* **21**, 45–51.
- Aatiq, A., Tigha, R. and Benmokhtar, S. (2012). "Structure, infrared and Raman spectroscopic studies of new $Sr_{0.50}SbFe(PO_4)_3$ and $SrSb_{0.50}Fe_{1.50}(PO_4)_3$ Nasicon phases," *J. Mater. Sci.* **47**, 1354-1364.
- Anantharamulu, N., Rao, K. K., Vithal, M. and Prasad, G. (2009). "Preparation, characterization, impedance and thermal expansion studies of $Mn_{0.5}MSb(PO_4)_3$ ($M = Al, Fe$ and Cr)," *J. Alloys Compd.* **479**, 684-691.
- Brown, I. D. and Altermatt, D. (1985). "Bond-valence parameters obtained from a systematic analysis of the inorganic crystal structure database," *Acta Crystallogr., Sect. B: Struct. Sci.* **B41**, 244-247.
- Butt, G., Sammes, N., Tompsett, G., Smirnova, A. and Yamamoto, O. (2004). "Raman spectroscopy of superionic Ti-doped $Li_3Fe_2(PO_4)_3$ and $LiNiPO_4$ structures," *J. Power Sources* **134**, 72-79.
- Delmas, C., Viala, J. C., Olazcuaga, R., Le Flem, G., Hagenmuller, P., Cherkaoui, F. and Brochu, R. (1981). "Ionic conductivity in Nasicon-type phases $Na_{1+x}Zr_{2-x}L_x(PO_4)_3$ ($L = Cr, In, Yb$)," *Solid State Ionics* **3/4**, 209-214.
- Hong, H. Y-P. (1976). "Crystal structures and crystal chemistry in the system $Na_{(1+x)}Zr_2Si_xP_{(3-x)}O_{12}$," *Mater. Res. Bull.* **11**, 173-182.
- Husson, E., Genet, F., Lachgar, A. and Piffard, Y. (1988). "The vibrational spectra of some antimony phosphates," *J. Solid State Chem.* **75**, 305-312.
- Padhi, A. K.; Nanjundaswamy, K. S.; Masquelier, C. and Goodenough, J. B. (1997). "Mapping

- of transition metal redox energies in phosphates with Nasicon structure by lithium intercalation,” *J. Electrochem. Soc.* **144**(8), 2581-2586.
- Rodriguez-Carvajal, J. (1997). “Fullprof, Program for Rietveld refinement,” Laboratoire Léon Brillouin (CEA-CNRS) Saclay France.
- Roy, R., Vance, E. R. and Alamo, J. (1982). “[NZP], A new radiophase for ceramic nuclear waste forms,” *Mater. Res. Bull.* **17**, 585-589.
- Shannon, R. D. (1976). “Revised effective ionic and systematic studies of interatomic distances in halides and chalcogenides,” *Acta Crystallogr., Sect.A: Cryst. Phys., Diffr., Theor. Gen. Crystallogr.* **32**, 751-767.
- Sudarsana, V., Muthe, K .P., Vyas, J. C. and Kulshreshtha, S. K. (2002). “PO₄ tetrahedra in SbPO₄ and SbOPO₄ : a ³¹P NMR and XPS study,” *J. Alloys Compd.* **336**, 119–123.
- Woodcock, D. A., Lightfoot, P. and Smith, R. I. (1999). “Powder neutron studies of three low thermal expansion in the NZP family: K_{0.5}Nb_{0.5}Ti_{1.5}(PO₄)₃, BaTi₂(PO₄)₃ and Ca_{0.25}Sr_{0.25}Zr₂(PO₄)₃,” *J. Mater. Chem.* **9**, 2631-2636.